MSU Fen Bil. Dergi., 9:1 817-826, 2021 MSU J. of Sci., 9:1 817-826, 2021
Araştırma Makalesi/ Research Article

An Evaluation on the Behaviors of Aftershock Sequence of November 26th, 2019 Earthquake, M_L=6.3, North of Durrës, Albania

Serkan ÖZTÜRK[1], Rrapo ORMENI[2]
[1]Gümüşhane University, Department of Geophysics, Gümüşhane, Turkey
[2]Institute of Geosciences Energy, Water and Environment, Polytechnic University of Tirana, Albania
: serkanozturk@gumushane.edu.tr, [1] 0000-0003-1322-5164, [2] 0000-0002-5514-2204

Received (Geliş): 18.03.2021 Revision (Düzeltme):29.04.2021 Accepted (Kabul): 03.05.2021

ABSTRACT

A comprehensive assessment of aftershocks occurrence for the November 26th, 2019 earthquake, M_L=6.3, 16 km north of Durrës, Albania was achieved. *b*-value was estimated as 0.88 ±0.07. *b*-value is close to 1.0 and relatively small *b*-value may be resulted from the plenty of larger aftershocks with $M_L \geq 4.0$. *p*-value was calculated as 1.23±0.08 with *Mmin*=3.1 and *Tstart*=0.0034 days. This high *p*-value may be a result of the relative fast decay rate of aftershock activity. *Dc*-value was calculated as 1.74±0.09 and it means that aftershocks are homogeneously distributed at larger scales. The smallest *b*-values and the largest *p*-values were observed in the north, northwest and northeast parts of the mainshock. The smaller *b*-values correlate with the larger stress variations, whereas the larger *p*-values are related to the maximum slip after mainshock. Consequently, region-time-magnitude analyses of the aftershocks occurrence may supply important clues for the fast evaluations of real time aftershock hazard.

Keywords: Albania, Durrës earthquake, aftershock, *b*-value, *p*-value, *Dc*-value

26 Kasım 2019, M_L=6.3, Kuzey Durrës, Arnavutluk Depreminin Artçı Şok Dizisinin Davranışları Üzerine Bir Değerlendirme

ÖZ

26 Kasım 2019, M_L=6.3, kuzey Durrës, Arnavutluk depreminin artçı şok oluşumunun detaylı bir değerlendirmesi yapılmıştır. *b*-değeri 0.88 ±0.07 olarak hesaplanmıştır. *b*-değeri 1.0'e yakındır ve nispeten küçük *b*-değeri $M_L \geq 4.0$ olan büyük artçı şokların fazla oluşundan kaynaklanmış olabilir. *p*-değeri, *Mmin*=3.1 ve *Tstart*=0.0034 gün alınarak 1.23±0.08 olarak hesaplanmıştır. Bu yüksek *p*-değeri artçı şok aktivitesinin nispeten hızlı azalım oranının bir sonucu olabilir. *Dc*-değeri 1.74±0.09 olarak hesaplanmıştır ve buda artçı şokların daha büyük ölçeklerde homojen olarak dağıldığı anlamına gelir. En küçük *b*-değerleri ve en büyük *p*-değerleri ana şokun kuzey, kuzeybatı ve kuzey kısımlarında gözlenmiştir. Daha düşük *b*-değerleri daha büyük gerilme değişişimler ile ilişkiliyken, daha büyük *p*-değerleri ana şoktan sonraki maksimum atım ile ilişkilidir. Sonuç olarak, artçı şok oluşumlarının bölge-zaman-magnitüd analizleri gerçek zamanlı artçı şok tehlikesinin hızlı değerlendirmeleri için önemli ipuçları sağlayabilir.

Anahtar Kelimeler: Arnavutluk, Durrës depremi, artçı şok, *b*-değeri, *p*-değeri, *Dc*-değeri

INTRODUCTION

A strong, M_L=6.3, earthquake near Durrës, Albania, occurred on November 26th, 2019 with the epicenter coordinates of 41.459°N and 19.442°E. The Institute of Geosciences, Energy, Water and Environment (IGEWE) reported that the earthquake occurred at 02:54:11 GMT (04:54:11 a.m. local time) around 39 km underground near the Hamallaj, northwest of Durrës and some 35 km west of Tirana, which is the strongest earthquake of the last 40 years. Some details of the mainshock occurrence was given in Table 1. It was followed minutes later by a series of weaker aftershocks, with the strongest measuring magnitude 5.5. Unfortunately, 51 people lost their lives. In Durrës district, 47 people were recovered from the ruins. The number of wounded reached about 760. More than 12,000 people remain homeless. The largest damages in the buildings were in the Durrës, in the district of Tirana as well as in the district of Lezha, damages have also occurred in the districts of Shkodra, Diber, Berat *etc*. Liquefaction phenomena was observed extensively in the area between the villages of Juba and Hamallaj. Strong earthquake occurrences in this part of the world can be resulted with human victims, property damage, and social and economic disruption as the African Plate moves northward towards Europe by 4-10 mm annually, with regular earthquakes occurring alongside the Eurasia-Africa plate boundary, mainly in Greece, Turkey, Sicily and Italy. There is reliable evidence that the old town of Durrës (Dyrrachium) has been stricken several times by strong earthquakes that have caused serious human and economic losses. Reports found in old chronicles show that this town has been almost totally destroyed in the years 177 B.C, 334 or 345 A.C., 506, 1273, 1279, 1869 and 1870.

Table 1. Detailed information of November 26th, 2019, north of Durrës mainshock. M_L: mainshock magnitude, Ma_{max}: the maximum aftershock magnitude and Ma_{min}: the minimum aftershock magnitude

Year	Month	Day	Origin Time (GMT)	Longitude	Latitude	Depth (km)	(M_L)	Ma_{max}	Ma_{min}
2019	11	26	02:54:11	19.442	41.459	39	6.3	5.5	0.9

The evidence of the earthquake of March, 1273 says that the town which had a population of 25 thousand people at that time was totally destroyed. On December of 1926, the town of Durrës and the surrounding region were hit by a series of strong earthquakes [1-7]. In recent years, several strong earthquakes occurred in and around Durrës, e.g., October 15th, 2016, July 3rd, 2017 and July 4th, 2018 earthquakes.

Aftershock sequences are generally considered as an important part of the earthquake occurrences since a strong mainshock can produce a large number of aftershocks in a short time and in a small region. Practical applications for the evaluation of aftershock occurrences can be preferred since large aftershock sequences may give some significant further seismic hazard assessments on the minimization of the human victims, property damage, and social and economic disruption [8]. For this reason, aftershock analyses have been gained more attention in recent years and many statistical studies on this subject by different authors for different aftershock sequences were achieved for different parts of the word [9-22]. Moreover, aftershock hazard assessment implies to statistically clarifying and forecasting the frequency that an aftershock in a certain level will occur. The modified Omori law [23] estimates the aftershock numbers after the mainshock. It is also necessary to combine this law with the Gutenberg-Richter [24] method to realize an aftershock probability evaluation. Also, fractal dimension of aftershock epicenter distributions is an effective tool to define the self-similar structure of aftershock occurrences and fractal dimension has widely been used in statistical seismology, especially for the measurements of complexity and stress distribution in the aftershock occurrence and aftershock clustering [25]. As stated in literature given above, region-time-magnitude behaviors of aftershock occurrences have significant information about the earthquake nucleation, fault geometry, material properties in the fault zone, as well as the distributions of stress, strength and temperature. It is well known that strong/large aftershock occurrences may have a potential to cause additional cumulative damage to structures since it is difficult to predict them. For this reason, evaluation of region-time-magnitude behaviors of the aftershocks is very important and interesting for protecting against and mitigating earthquake disasters. Thus, many statistical models have been suggested to define the spatial and temporal aftershock properties.

The main purpose of this study is to provide a detailed region-time-magnitude evaluation including several aftershock parameters such as the *b*-value of the frequency-magnitude distribution, the *p*-value of the modified Omori law and *Dc*-value of the fractal dimension for 910 aftershocks identified in seven months after the mainshock. For the calculations of aftershock parameters of north Durrës earthquake that occurred on November 26th, 2019 in Tirana district of Albania, ZMAP software package [26] was used. The results obtained in this study have a significance not only for the region-time-magnitude behaviors of the aftershock sequence but also help to understand the generation of aftershock occurrences. Statistical properties of aftershocks also make a contribution to attempts to forecast aftershock activities following large mainshocks and can be used to reveal the seismic hazard in this region.

Aftershock Data for November 26th, 2019 Durrës Earthquake

A detailed region-time-magnitude evaluation of aftershock sequence of the November 26th, 2019, a strong earthquake (M_L6.3) occurred about 16 km north of the Durrës city in the Adriatic Sea, Albania was achieved in this study. The data used in this study were compiled from the Albanian Seismological Stations, Montenegro Seismological Stations and from INGV, MEDNET, and AUTH networks. Complete and homogenous catalog of aftershock data were provided for the mainshock with local magnitude M_L=6.3, occurred at 41.459°N and 19.442°E, and at 02:54:11 GMT on November 26th, 2019. The aftershock catalog includes approximately a period of over seven months, that is from the time of the mainshock (November 26th, 2019) until June 30th, 2020. A total of 910 aftershocks with magnitude M_L larger than and equal to 0.9 were used in a time period of about 215 days. The earthquake of November 26th, 2019 and its aftershocks were recorded by permanent broadband seismological stations that are part of the Albanian Seismological Network (bci, puk, dhr, php, vlo, kbn, lsk, bpa1, bpa2 and srn), as well as by the neighbouring seismic networks, namely, AUTH (fna, igt, nest, the, lkd2, mev), MSO (pdg, bey, bry, bdv, hcy, nky, pvy, ulc), INGV (mrvn, noci, scte, sgrt) and MEDNET (tir). The epicentres were located using P and S onsets, a local velocity model [27] and the Hypo inverse program [28]. The smallest magnitude events 0.9 to 3.0 (Richter) are recorded at least by the closest stations to the epicenters (dhr, tir, bpa1, bpa2, ulc, etc).

The epicenter locations of aftershocks were drawn in Figure 1 and the cumulative number of aftershocks in about a time period of seven months was plotted in Figure 2a. In order to analyze the temporal magnitude distribution, magnitude versus time changes of aftershocks was plotted in Figure 2b. Time-magnitude changes of aftershock occurrences were drawn in time interval about 215 days. As seen in Figure 2b, the largest aftershock with M_L=5.5 observed in about three hours after the mainshock. However, aftershock occurrences larger than M_L=4.0 show two increases on the 23th and 64th days after the mainshock. There are also some aftershocks whose magnitudes varies from 4.0 to 5.0 in 25 days after the mainshock. A decreasing trend in the number of aftershocks with magnitude M_L=3.0 can be shown after the first two months from the mainshock, and magnitude of aftershocks generally varies from 1.0 to 3.0 in the rest of aftershock period. It is well known that aftershock occurrences show elliptical distribution that spread in different directions from the mainshock epicenter [23]. Therefore, all these shocks and subsequent events that fall in this area can be accepted as aftershocks. Also, many authors suggested different time intervals for aftershock duration, from one month to one year [8, 10, 14, 23]. Hence, we identified the region and time interval of Durrës aftershocks by considering these literature studies.

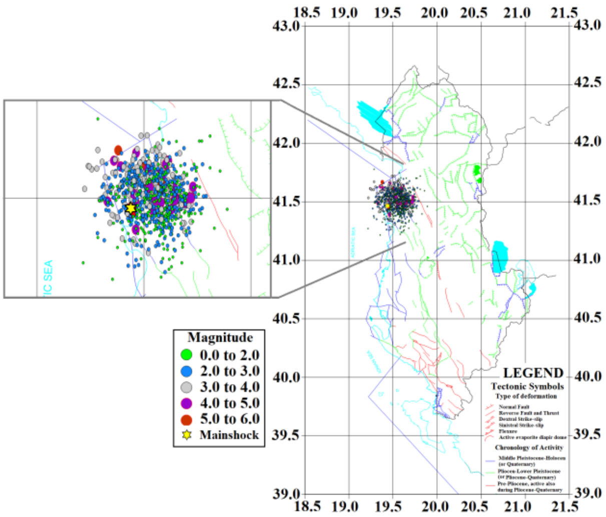

Figure 1. Epicenter distribution of the aftershocks of November 26th, 2019 north of Durrës earthquake. Different magnitude sizes of the aftershocks were given by different symbols

Methods and Brief Description of the Parameters

There are many statistical models to analyze the behaviors of aftershock occurrences, however, an aftershock sequence can be described in region (fractal dimension [29], time (modified Omori law) [30] and magnitude (Gutenberg-Richter law) [24]. Since the aftershocks can supply important and reliable information about the fault structure, cracks distribution, earthquake migration and the state of stress in the crust, these power-law distributions are the most common in the evaluation of aftershock sequence.

The cumulative earthquake-magnitude distribution in any region is described with the Gutenberg and Richter [24] relation (G-R). This power-law distribution between the frequency and magnitude of aftershocks can be explained with the following equation:

$$\log_{10} N(M) = a - bM \quad (1)$$

where *N(M)* is the cumulative number of aftershocks with magnitudes larger/equal to *M*, *a* and *b*-values are positive constants. *a*-value represents the seismicity level and shows differences from region to region since it depends on data period and study area. *b*-value shows the frequency- magnitude distribution of aftershocks, and tectonic structure and stress distribution of investigated area effects the spatio-temporal changes of *b*-value. The estimated *b*-value is generally between 0.6 and 1.4 [10].

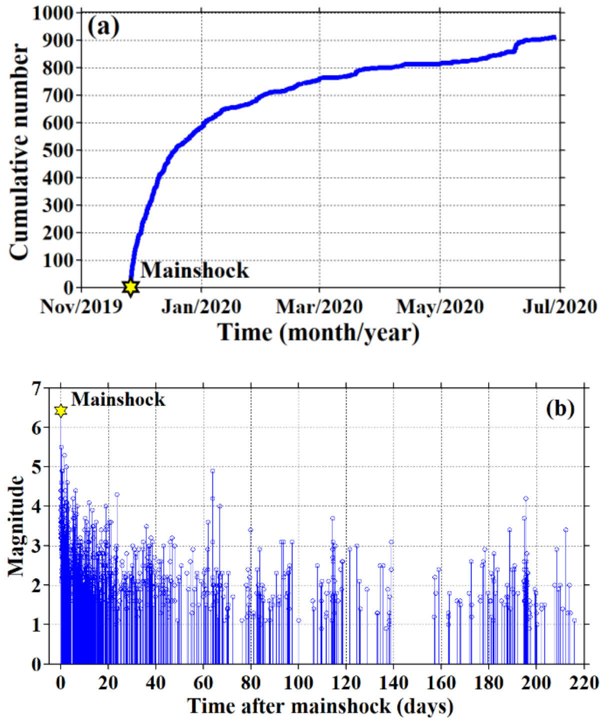

Figure 2. a) Cumulative number of aftershock in seven months after the mainshock. **b)** Magnitude variations of aftershock sequence as a function of time

However, *b*-value is roughly between 0.3 and 2.0, depending on the study area [31]. Frohlich and Davis [32] suggested that the mean *b*-value in global scale can be given as equal to 1.0.

Temporal decay rate of aftershocks can be empirically defined by the modified Omori law (MO). The number of aftershocks increases suddenly after the mainshock and then shows a decreasing trend with time after the mainshock according to the MO law. This power-law distribution can be given with the following formula:

$$n(t) = \frac{K}{(t+c)^p} \quad (2)$$

where *n(t)* is the aftershocks occurrence rate (number of aftershocks/day) per unit time, *t*-days after the mainshock. *K*, *p*, and *c* values are empirically obtained positive constants, and they depend on the total number of aftershocks in the sequence and the activity rate in the earliest part of the sequence, respectively. *K*-value depends on the total number of events, *c*-value on the rate of activity in the earliest part of the sequences. *c*-value changes between 0.02 and 0.5 and all the reported positive *c*-values result from incompleteness [33]. Among these three parameters, *p*-value is decay parameter and the most significant. Many researchers suggested that *p*-value usually changes between 0.5 and 1.8 for different aftershock sequences [10, 30]. Thus, these changes may be related to the tectonic situations of the region such as stress, fault heterogeneity, coseismic deformation, slip distribution and crustal heat flow [13].

Fractal concept has been used for a long time in order to describe the complexity of fault systems in which is observed the region and laboratory. One of the most commonly used methods for the estimation of fractal dimension is the correlation integral technique owing to its greater reliability and sensitivity to small variations in clustering features of points such as epicenters. Fractal dimension of the epicenter distribution of aftershocks can be modelled by using two-point correlation dimension, *Dc*, and correlation sum *C*(*r*) formulated by following equation [29]:

$$Dc = \lim_{r \to 0}\left[\log C(r) / \log r\right] \tag{3}$$

$$C(r) = 2N_{R<r} / N(N-1) \tag{4}$$

where *C*(*r*) is the correlation function, *r* is the distance between two epicenters and *N* is the number of aftershocks pairs separated by a distance *R*<*r*. If epicenter distribution has a fractal structure, following equation can be given:

$$C(r) \sim r^{Dc} \tag{5}$$

where *Dc* is a fractal dimension, more definitely, the correlation dimension. Fractal dimension changes between 0 and 2 related to the seismically and tectonically active regions. If *Dc*-value is close to zero, it can be evaluated as all aftershocks clustered into one point. If *Dc*-value is close to 1, it shows the dominance of line sources. If *Dc*-value is close to 2, it indicates the planar fractured surface being filled-up and it is suggested that the earthquake epicenters are homogeneously distributed over a two-dimensional fault plane. If *Dc*-value is close to 3, it means that earthquake fractures are filling up a crustal volume. Fractal dimension may be estimated in order to avoid the possible unbroken fields, and these unbroken regions are suggested as potential seismic gaps to be broken in the future [25]. Also, it has been observed in many studies that there is a negative correlation between *Dc*-value and *b*-value. Larger *Dc*-value associated with smaller *b*-value is the dominant structural feature in the regions of increased complexity in the active fault system. Moreover, it can be an indication of stress changes in the region [34, 35].

RESULTS and DISCUSSIONS

In this study, an assessment of region-time-magnitude behaviors of aftershock sequence of November 26th, 2019 north of Durrës earthquake was performed by analyzing several seismotectonic parameters related to aftershock hazard evaluation in and around the aftershock area. One of the most significant steps can be given as the minimum magnitude of completeness, *Mc*-value, based on the assumption of the G-R size-scaling distribution of earthquakes. Magnitude completeness, *Mc*-value, can be defined as the minimum magnitude of complete reporting and it means that *Mc* level includes 90% of the earthquakes [36]. *Mc*-value shows spatio-temporal changes according to different networks and catalogs. Therefore, temporal changes in this value can potentially cause incorrect *b* and *p*-value estimations. *Mc*-value will be large in the early part of the aftershock sequence since small events may not be recorded during the first highest activity after the mainshock and, this large value may cause incorrect estimations on statistical analyses [10]. *Mc*-value as a function of time can be calculated rapidly and safely by considering the goodness of fit to a power law. Temporal change of *Mc*-value is provided by using a moving time window approach with the maximum likelihood method (for details, see Wiemer and Wyss, [36]).

For the aftershock sequence of north of Durrës earthquake, an overlapping moving window technique (provided with ZMAP) was used to see *Mc*-value variations in time, starting at the mainshock time. A sample window consisting of 10 aftershocks was chosen to plot the temporal *Mc*-value changes. Temporal variations in *Mc*-value was drawn in Figure 3. *Mc*-value is the largest at the beginning of the sequence (in the first ten hours) and changes between 3.0 to 4.0. Then, it decreases to about between 2.0 and 3.0 after a few days from the mainshock. *Mc*-value generally changes between 1.5 and 2.5 after 20 days from the mainshock.

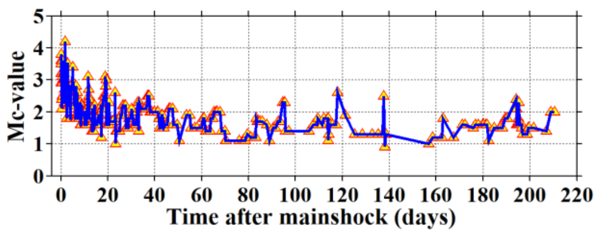

Figure 3. Temporal variations of magnitude completeness, *Mc*. *Mc*-value was estimated with a temporal overlapping windows, consisting of 10 aftershocks

Therefore, we suggest that *Mc*-value in the aftershock sequence does not show a stable value in time interval of seven months. In order to understand how much *Mc*-value changes depend on the sample size, different sample sizes such as 25, 75 and 100 events/window were tested for aftershock sequence and it was concluded that the selection of the sample size does not affect the results. Thus, temporal fluctuations in *Mc*-value shown in Figure 3 do not depend on the small sample size and *Mc*-value was taken as 2.7 in the estimation of *b*-value.

For the evaluation of variations in the number of aftershocks in different magnitude levels, magnitude histogram of the aftershock sequence was plotted in Figure 4a. Aftershock magnitudes changes between 0.9 to 5.5 and show a decrease in their numbers from the lower to higher magnitudes. As seen in magnitude histogram, the size of the many aftershocks varies from 1.0 to 4.0 and a maximum was observed in M_L=2.7. There are 291 events with magnitude M_L<2.0, 428 aftershocks 2.0≤M_L<3.0, 158 aftershocks 3.0≤M_L<4.0, 30 aftershocks 4.0≤M_L<5.0, 3 aftershocks 5.0≤M_L and, the aftershock with M_L=5.5 is the largest of all. As a result, the aftershock occurrences with magnitudes between 1.5 and 3.5 are more dominant in the aftershock region. Also, in order to see the variations in the number of aftershocks in different time intervals, time histogram of the events was plotted in Figure 4b. There is a large aftershock activity in the first two days and the number of aftershocks in this time interval is about 150. There is also a decrease in the number of aftershocks after 20 days. Then, average number of aftershocks decreases in time according to the modified Omori law (hyperbola on Fig. 4b). A stableness can be clearly seen after the first month and, the average number of aftershocks after the first month is less than 20. However, there is an increase in the number of aftershocks in the 195th (35 events) day. Thus, these types of evaluations can give preliminary results for the statistical properties of aftershock sequence which is associated with the aftershock probability evaluation and aftershock hazard in Durrës region of Albania.

A detailed region-time-magnitude evaluation of aftershock behaviors based on the statistical models aims to define the problem of determining whether or not it is possible to immediately and correctly find the aftershock parameters such as *K*, *c*, *p*, *b* following a mainshock [37]. If the average values of these parameters for the aftershock sequence are known, there can be a probability that existing values can be used reliably as preliminary data until the real data is available. Therefore, these scaling parameters were compared by combining the G-R and MO formulas and, their application range was studied for the aftershock sequence of November 26th, 2019 north of Durrës earthquake. The maximum likelihood estimation was used in the estimation of *b*-value in G-R relationship since it yields a more robust calculation than least square method [38]. On the assumption that the earthquake activity follows a non-stationary Poisson process [37], parameters in the MO formula can be calculated correctly by the maximum likelihood method.

Cumulative frequency-magnitude relation and decay rate of north of Durrës aftershock sequence were shown in Figure 5a and 5b, respectively. Based on the time variations in Figure 3, *Mc*-value was considered as 2.7. *b*-value and its standard deviation, as well as the *a*-value of G-R relation, were computed with the maximum likelihood method. For the aftershock sequence, *b*-value was computed as 0.88±0.07 with this *Mc*-value (Figure 5a). This *b*-value can be considered as relatively small but obtained *b*-value for aftershock sequence is close to 1.0. Thus, aftershock sequence matches the general feature of aftershocks such that frequency-magnitude distribution of aftershocks is represented by the G-R law with a *b*-value typically close to 1 [32].

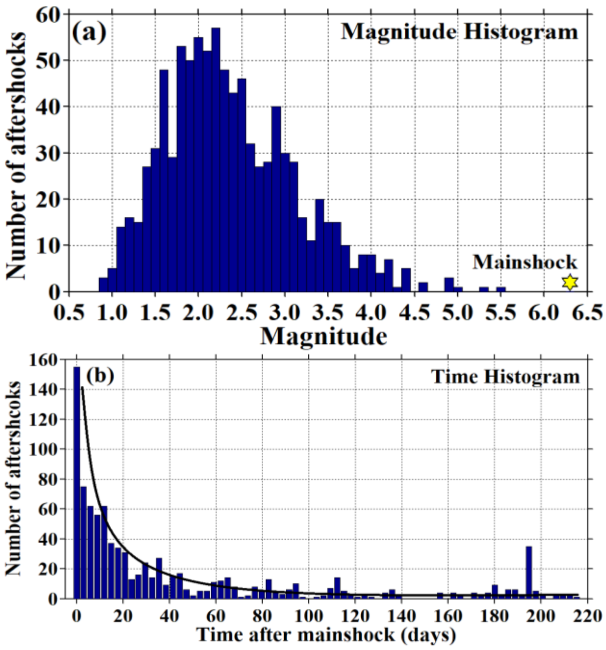

Figure 4. For the aftershock sequence of November 26th, 2019 north of Durrës earthquake: **a)** magnitude histogram, **b)** time histogram

As mentioned in Frohlich and Davis [32], low *b*-value may be explained with the low heterogeneity degree of medium, the high stress concentration or high strain in the aftershock area. Also, a small *b*-value shows a large proportion of aftershocks with large magnitudes. There are 188 aftershocks with magnitude 3.0≤M_L<5.0 and 3 events with magnitude M_L≥5.0. Thus, this relatively law *b*-value may be resulted from abundance of aftershocks with magnitude M_L≥4.0.

In order to provide the completeness in the catalog and to estimate the decay parameters of aftershock sequence, two important threshold values must be set: (i) a minimum magnitude threshold, *Mmin* and (ii) a minimum time threshold, *Tstart* (T_1), i.e. excluding the first hours to days from the analysis. As a simple application, *Mmin* can be arranged for the shortest *Tstart*.

However, this application uses the largest *Mc*-value defined for the earliest part of the aftershock sequence [10] and, this selection decreases the available number of data. To estimate the decay parameters of the modified Omori law for north of Durrës aftershock sequence, *Mmin*=3.1 and *Tstart*=0.0034 were considered. *c*-value is measured in time units, days for example. After some earthquakes, there is some small delay in the aftershock sequences. In some sequences, however, it can be observed a large incompleteness in the catalog at the very beginning of the aftershock sequence and therefore, an artificial large *c*-value may be estimated.

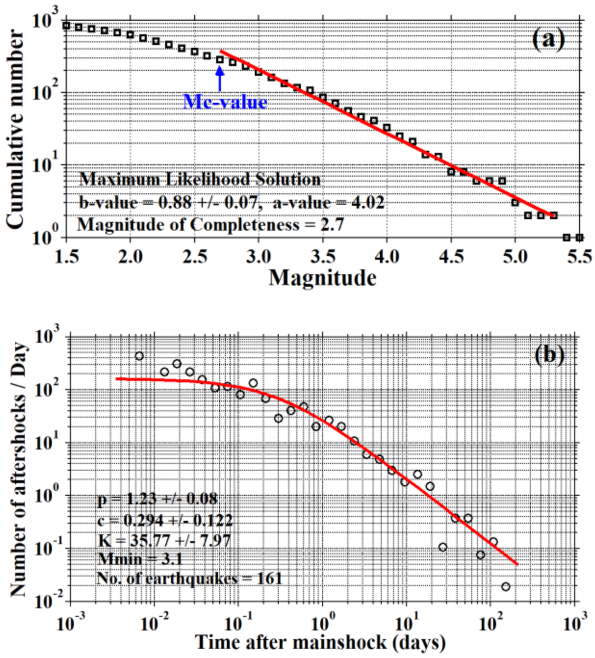

Figure 5. a) Gutenberg-Richter relation of aftershock sequence. *b*-value, its standard deviation, *Mc*-value as well as the *a*-value in the Gutenberg-Richter relation are given. **b)** Modified Omori model and decay parameters aftershock activity of north of Durrës (for the cases: $M_L \geq 3.1$) earthquake. Aftershock parameters such *p, c* and *K*-values in the modified Omori formula, the minimum magnitude and the number of aftershocks were also given

These types of uncertainties on the estimations were tried to be removed by taking *Mmin*=3.1 and *Tstart*=0.0034. In this way, although the number of aftershocks was largely decreased, the earliest part of the sequence was included in the analyses and completeness was provided. The effects of different *Mmin* and *Tstart* were tested in order to see the confidence of the results for *p* and *c*-values. All estimations were given in Table 2. Thus, for the estimation of decay parameters, 161 aftershocks with magnitude $M_L \geq 3.1$ were used (rectangular area, No: 25). Figure 5b shows the decay rate of aftershock activity versus time after the mainshock for aftershocks with magnitude *Mc*≥*Mmin* for the north of Durrës aftershock sequence. The *p*, *c* and *K*-values were estimated by using the maximum likelihood method with magnitude *Mc*≥*Mmin* and the occurrence rate was modeled by the MO formula. *p*=1.23±0.08, relatively larger than the global *p*-value 1.0, was calculated for aftershock sequence considering minimum magnitude *Mc*≥*Mmin*=3.1, T_1=0.0034 day since the number of aftershock is the maximum for a suitable *c*-value. *c*-value and *K*-value were calculated as 0.294±0.122 and 35.77±7.97, respectively. High *p*-value for a given aftershock sequence indicates a fast decay of aftershock activity and thus, the occurrence of aftershocks in north of Durrës earthquake shows a fast decay rate. Since the high *p*-value may be caused from the high stress heterogeneity [39, 40], we can conclude that there may be stress heterogeneity in the aftershock region. Detailed tests were made for decay parameters by using different *Mmin* (ranging from 2.7 to 3.6) and *Tstart* values (ranging from 0.0034 to 0.1). We saw that the *p*-value varies from 1.16 to 1.38 for different *Mmin* and *Tstart*, *c*-value between 0.025 and 1.122. Thus, as shown in Table 2, *p*-value has a characteristic that is in and around 1.2 and, *c*-value is suggested to strongly related to the *Mmin* in comparison with *p*-value.

Several statistical models have been applied to analyze the decay rate of aftershocks and to define the behaviors of aftershock sequences as a power law. Although alternative models such as Epidemic Type Aftershock Sequence (ETAS) model, stretched exponential relaxation, modified Omori law including a background rate term [9, 11, 14, 22, 37, 39] *etc*., have been supplied to evaluate the aftershock decay rate, different techniques have limited results relative to the modified Omori law. Among different techniques, the modified Omori law is one of the most effective approaches, and aftershock time series analyzed in this study are all well fit with the modified Omori model. Hence, and also considering the detailed statistics given in Table 2 (as seen in test 25), the modified Omori law seems suitable to model the decay rate of Durrës aftershock sequence.

The number of aftershocks may not be counted fully at the beginning of a sequence when smaller aftershocks are often hidden by larger ones due to overlapping and hence, too large *c*-value may be obtained. If all shocks can be counted, *c*-value may be zero [31]. There are two ideas in relation to *c*-value: one is that *c*-value is actually 0 and all the reported positive *c*-values result from incompleteness in the early stage of an aftershock sequence. The second opinion is that positive *c*-value can be obtained [33]. If *c*=0, *n (t)* in Equation (2) diverges at *t*=0. If the enlargement of the aftershock area occurs in an early stage, a relatively high *c*-value may be computed [30]. Also, for the aftershock sequences following relatively small mainshocks, estimated *c*-values are generally small (*c*≤0.01 days). Hirata [33] stated that *c*-value changes between 0.02 and 0.5 for the 1969 Shikotan-Oki earthquake. Considering these detailed literature studies, we can conclude that the use of *Mmin*=3.1 and *Tstart*=0.0034 day for the estimation of decay parameters seems better to fit the north of Durrës aftershock sequence. These results are in accordance with other studies and also suggest that aftershock activity does not have a heterogeneous background seismicity pattern. Thus, the simple modified Omori model appears suitable to describe the aftershock decay parameters in north of Durrës earthquake sequence.

Figure 6 shows the fractal dimension of aftershock epicenter distributions for north of Durrës earthquake. *Dc*-value was calculated by fitting a straight line to the curve of mean correlation integral against the epicenter distance, *R* (km). *Dc*-value was computed as 1.73±0.10

Table 2. Some tests on the input values for the estimation of aftershock decay parameters

No	*Tstart* (T_1, day)	*Mmin*	Time interval (*t*, day)	Number of aftershocks used	*p*-value	*c*-value	*K*-value
1	0.05	2.7	0.052083≤*t*≤212.2076	277	1.34±0.09	1.122±0.369	119.86±36.01
2	0.05	3.0	0.052083≤*t*≤212.2076	182	1.30±0.09	0.595±0.246	57.86±16.5
3	0.05	3.3	0.052083≤*t*≤212.2076	108	1.38±0.12	0.48±0.24	35.99±12.44
4	0.05	3.4	0.061111≤*t*≤212.2076	97	1.32±0.12	0.42±0.239	28.75±9.98
5	0.05	3.5	0.061111≤*t*≤195.5188	78	1.27±0.11	0.206±0.15	17.7±5.46
6	0.05	3.6	0.061111≤*t*≤195.5188	65	1.22±0.11	0.122±0.116	12.51±3.69
7	0.1	2.7	0.10972≤*t*≤212.2076	272	1.34±0.09	1.099±0.386	118.33±36.32
8	0.1	3.0	0.10972≤*t*≤212.2076	177	1.29±0.09	0.569±0.264	56.78±16.74
9	0.1	3.3	0.10972≤*t*≤212.2076	104	1.37±0.12	0.44±0.255	34.61±12.34
10	0.1	3.4	0.10972≤*t*≤212.2076	94	1.31±0.12	0.387±0.253	27.81±9.92
11	0.1	3.5	0.10972≤*t*≤195.5188	75	1.22±0.11	0.108±0.13	15.24±4.46
12	0.1	3.6	0.10972≤*t*≤195.5188	62	1.16±0.10	0.025±0.093	10.47±2.89
13	0.01	2.7	0.015278≤*t*≤212.2076	284	1.31±0.08	0.924±0.293	105.58±28.25
14	0.01	3.0	0.015278≤*t*≤212.2076	189	1.26±0.08	0.458±0.178	51.1±12.56
15	0.01	3.1	0.015278≤*t*≤212.2076	159	1.23±0.08	0.304±0.132	36.21±8.33
16	0.01	3.2	0.015278≤*t*≤212.2076	131	1.35±0.10	0.339±0.145	35.54±9.41
17	0.01	3.3	0.015278≤*t*≤212.2076	115	1.31±0.10	0.284±0.134	28.11±7.42
18	0.01	3.4	0.015278≤*t*≤212.2076	104	1.24±0.09	0.222±0.117	22.07±5.62
19	0.01	3.5	0.015278≤*t*≤195.5188	84	1.23±0.10	0.146±0.088	15.78±3.91
20	0.01	3.6	0.015278≤*t*≤195.5188	69	1.23±0.10	0.144±0.097	12.87±3.51
21	-	2.7	0.0034722≤*t*≤212.2076	286	1.30±0.08	0.888±0.278	103.01±26.84
22	-	2.8	0.0034722≤*t*≤212.2076	259	1.26±0.07	0.656±0.218	77.86±18.69
23	-	2.9	0.0034722≤*t*≤212.2076	231	1.25±0.07	0.507±0.178	62.35±14.27
24	-	3.0	0.0034722≤*t*≤212.2076	191	1.26±0.08	0.44±0.166	50.18±11.95
25	**-**	**3.1**	**0.0034722≤*t*≤212.2076**	**161**	**1.23±0.08**	**0.294±0.122**	**35.77±7.97**
26	-	3.2	0.0034722≤*t*≤212.2076	133	1.34±0.09	0.327±0.134	34.92±8.92
27	-	3.3	0.0034722≤*t*≤212.2076	117	1.30±0.09	0.267±0.12	27.35±6.88
28	-	3.4	0.0034722≤*t*≤212.2076	106	1.23±0.09	0.202±0.101	21.31±5.11
29	-	3.5	0.0034722≤*t*≤195.5188	86	1.22±0.09	0.138±0.076	15.49±3.63
30	-	3.6	0.0034722≤*t*≤195.5188	71	1.21±0.10	0.124±0.077	12.32±3.08

for epicenter distribution of 910 aftershocks with 95% confidents interval by the least squares method. This log-log relation shows a clear linear range and scale invariance in the self-similarity statistics between 5.03 and 62.28 km (indicated in Figure 6 as "Range"). If there is an increasing complexity in the active fault system with larger *Dc*-value and lower *b*-value, the stress release occurs on fault planes of smaller surface area [34]. Larger *Dc*-value is also sensitive to heterogeneity in magnitude distribution. *Dc*-value estimated as 1.73±0.10 in this study suggests that aftershocks are more clustered at larger scales or (in smaller areas) and this relatively high *Dc*-value may be a dominant structural characteristic for aftershock region. Since *Dc*-value is close to 2.0, we can imply that north of Durrës aftershocks are homogeneously distributed. Also, the heterogeneity of stress field controls the region [25]. Hence, it can be stated a non-heterogeneous stress distribution in north of Durrës region. Thus, we can statistically analyze and define the spatial distributions of aftershock epicenters and their fracture systems with fractal behaviors.

For the regional changes of *b*-value and *p*-value, a spatial grid of points with a nodal separation of 0.01° in longitude and latitude was used. The number of nearest epicenters (*Ne*) were taken as 400 for each node and the number of minimum nearest epicenters (minimum number of events > *Mc*), *Nemin*, were taken as 100. Then, the regional distributions of *b*-value and *p*-value were imaged by using these values with color nodes on the maps. An important assumption is that *c*-value was selected as 0.294 days and *Tstart*=0.0034 day for the representation of *p*-value in the modified Omori formula since these values are more satisfying (as seen in Table 1) to image the regional changes.

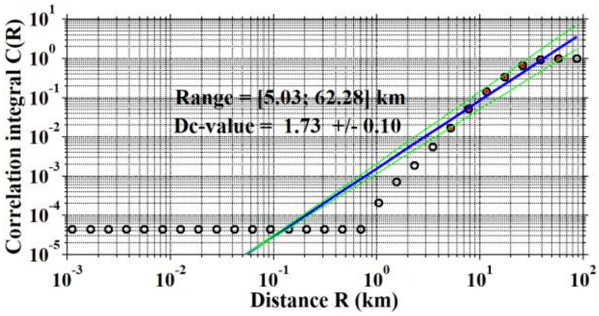

Figure 6. Fractal dimension, *Dc*-value, for north of Durrës aftershock sequence. Scale invariance in the self-similarity statistics was given as "Range"

Both *b*-value and *p*-value regional maps were created by using the same grid and number of aftershocks in each grid node, and the maximum likelihood method was used in the estimation of these two parameters.

Figures 7a and 7b show the regional distributions in *b*-value and *p*-value for north of Durrës aftershock sequence, respectively. Regional variations in *b*-value changes between 0.4 and 0.9, and *p*-value shows a distribution from 0.7 and 1.3. Considering the change interval in *b*-value and *p*-value according to several researchers such as Utsu [31], Wiemer and Katsumata [10], Öztürk et al., [14], Enescu et al., [15], Ansari [19], Öztürk and Şahin [21] etc., a general result is that changes in *b*-value and *p*-value for north of Durrës aftershock sequence are accordance with these results. Aftershock activity of north of Durrës sequence is densely distributed in the north, east, northeast and northwest parts of mainshock epicenter. The aftershocks with magnitude $3.0 \leq M_L < 4.0$ were observed in these parts of the study region (as seen in Figure 1). Also, the larger aftershocks whose magnitude varies from 4.0 to 5.0 show an intense distribution from the mainshock epicenter to the east, west and northwest directions. The *b*-values smaller than 1.0 were generally observed in all parts of the study region. However, the smallest *b*-values (<0.6) were calculated in the north, northwest and northeast parts of the mainshock. These smallest *b*-values were generally observed in the larger aftershock ($M_L \geq 4.0$) regions whereas the other large *b*-values are related to the area in which small shocks ($M_L < 3.0$) generally occurred. The *p*-values for north of Durrës aftershock sequence show both small and great variations in all the study region. The larger *p*-values (>1.0) were observed in the north, northwest and northeast parts of the mainshock epicenter and the activity in these parts shows faster decay of aftershock activity. However, the lower *p*-values (<0.9) regions are observed related to the south, west, east, southwest and southeast parts of the study region. This result gives the appearance that decay is slower than the other parts at these parts of the region. Consequently, decay rates of aftershock activity in the northern, southwestern and southeastern ends of the sequence (p~0.7) are much slower than that of along the north, northwest and northeast parts.

Region-time-magnitude analyses of aftershock sequence may supply preliminary results for the evaluation of reliable probability and hazard of an aftershock region. As mentioned above, there is a clear relation between these aftershock parameters and the tectonic condition of the aftershock area such as stress and slip distribution, surface heat flow and structural heterogeneity. Studies show that stress relaxation in the fault zone materials causes higher temperatures in the aftershock source zone and leads to a larger *p*-value. Also, it is suggested that regional changes of *b* and *p*-values are related to the slip distribution during the mainshock. A general result from literature studies that smaller *b*-value changes are related to lower stress distribution after the mainshock and larger *p*-values correlate with the regions that experienced higher slip during mainshock. Consequently, these results show that both *b*-value and *p*-value can be used in the aftershock probability evaluation, and regional changes of these parameters have an important influence on aftershock hazard assessments.

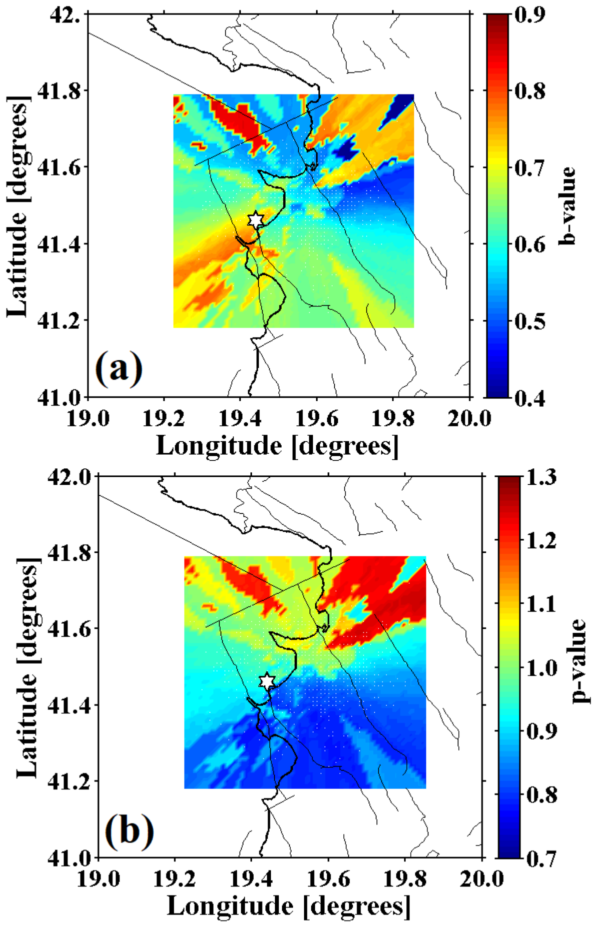

Figure 7. Regional changes of: **a)** *b*-value, **b)** *p*-value. *b*-value and *p*-value were plotted by sampling the nearest 400 aftershocks for each node of a grid with nodal separation of 0.01°. Star represents the mainshock

In recent years, many authors made illuminating studies which are focused on these types of aftershock evaluations, especially on *b*-value and *p*-value analyses for different aftershock occurrences. Temporal properties of 39 aftershock sequences in southern California were evaluated by Kisslinger and Jones [41] and they suggest a direct relationship between surface heat flow and *p*-value. Regional variations of *b* and *p*-values for the Landers, Northridge, Morgan Hill and Kobe aftershock sequences was analyzed by Wiemer and Katsumata [10], and they suggested that regional distributions of *b*-value and *p*-value are correlated with the slip distribution during the mainshock, and the largest slip regions are related to large *b*-value. Comprehensive statistical assessments for the spatio-temporal behaviors of different aftershock sequences from Japan and Turkey were achieved by Bayrak and Öztürk [13], Öztürk et al., [14], Enescu et al., [15], Öztürk and Şahin [21] and Nanjo [22]. According to their results, there is a general relationship among the regional changes of *b* and *p*-values, the rupture mechanism and material properties of an aftershock region. They resulted that lower *b*-value changes are related to lower stress distribution after mainshock and higher *p*-values correlate with the areas that experienced larger slip during mainshock. These studies show that evaluation of aftershock sequences may benefit for earthquake hazards mitigation in the form of rapid assessment for short-term earthquake hazards immediately after the strong/large earthquakes. Also, spatio-temporal patterns in aftershock activity may indicate rapid change of mainshock-induced stress fields and may point out a strong aftershock triggered by the mainshock. Thus, obtained results in the present study may be important and give preliminary perspective for mainshock-aftershock pattern to earthquake hazard evaluation since there is not many detailed studies in literature on November 26th, 2019 north of Durrës, Albania, strong earthquake and its aftershocks.

CONCLUSIONS

A comprehensive statistical region-time-magnitude evaluation for the aftershock sequence of November 26th, 2019, M_L=6.3, north of Durrës, Albania, earthquake was achieved. For this purpose, the *b*-value from Gutenberg-Richter relation, *p*-value from modified Omori law, *Dc*-value from fractal dimension as well as the expected number of aftershocks and aftershock occurrence probability for different magnitude sizes in the aftershock sequence were analyzed. Earthquake data including 910 aftershocks in seven months after the mainshock was taken from the Albanian Seismological Stations, Montenegro Seismological Stations and from INGV, MEDNET, and AUTH networks. Magnitude completeness for aftershock sequence was taken as *Mc*=2.7 and *b*-value was estimated as 0.88±0.07. This *b*-value is relatively close to 1.0 and this aftershock sequence is well represented by the Gutenberg-Richter relation. This relatively small *b*-value may be related the plenty of larger aftershocks with $M_L \geq 4.0$. *p*-value was estimated as 1.23±0.08 with a *c*-value=0.294±0.122 by fitting the data for events with *Mmin*=3.1 and *Tstart*=0.0034. A relatively large *p*-value was calculated since aftershock activity shows a relatively fast decay rate. These results also indicate that no background activity is not included in the estimation and there is not an incompleteness at the beginning of the sequence according to this *c*-value. Therefore, the simple modified Omori law can be considered a suitable model for north of Durrës aftershock sequence. *Dc*-value was estimated as 1.73±0.10 and it can be concluded that the north of Durrës aftershocks are not heterogeneously distributed over a two dimensional fault plane. Also, there may be an increasing complexity in the aftershock area with these large *Dc*-value and small *b*-value.

Regional variations of *b*-value change between 0.4 and 0.9. In general, aftershock region has small *b*-values, however, the lowest *b*-values were observed in the north, northwest and northeast parts of the mainshock. These smallest *b*-values correlate with the larger aftershock ($M_L \geq 4.0$) regions. Regional changes in *p*-value vary from 0.7 to 1.3. The largest *p*-values were also observed in the north, northwest and northeast parts of the mainshock epicenter and aftershock activity in these parts shows fast decay rate. On the other hand, since there is no information on slip distribution, stress changes and coseismic deformation for aftershock region, we could not make a suitable and reliable assessment among *b*-value, *p*-value and rupture mechanism of the aftershock region. Also, since no information on surface rupture of the causative faults were not stated in north of Durrës aftershock region, we did not suggest a relationship between slip and *p*-value. These results show that an effective region-time-magnitude evaluation of aftershock sequence may be important and these types of preliminary assessments of aftershock occurrences may be crucial for a contribution of disaster protection measurements and the fast evaluations of real time aftershock hazard in a short-time immediately following strong/large earthquakes in this part of Albania.

ACKNOWLEDGEMENT

The authors would like to thank to reviewers for their useful and constructive suggestions in improving this paper. The new release of *ZMAP* software is freely available (version 7, https://github.com/zmap/zmap). We are grateful to Albanian Seismological Stations, Montenegro Seismological Stations and from INGV, MEDNET, and AUTH networks for providing us aftershock catalog.

REFERENCES

[1] Sulstarova E., Koçiaj S. The Albania Earthquake Catalog. Edition of Academy of Sciences of Albania, 1975.

[2] Sulstarova E., Kociaj S., Aliaj Sh. Seismic regionalization of PSR of Albania. Publishing House of “8 Nentori” Tirana, 1-297, 1980.

[3] Jolivet L. Faccenna C. Mediterranean extension and the Africa-Eurasia collision, Tectonophysics, 19:6 1095-1106, 2000.

[4] Aliaj Sh., Sulstarova E., Muço B., Koçiu S. Seismotectonic map of Albania at the scale 1:500.000, Instituti i Sizmologjisë Tiranë, 2000.

[5] Aliaj Sh., Koçiu S., Muço B., Sulstarova E. Seismicity, seismotectonic and seismic hazard assessment in Albania, Published by Albanian Academy of Sciences, 2010.

[6] Aliaj Sh., Meço S. Neotectonics map of Albania at the scale 1:200.000, Albanian Geological Survey, Tirana, 2018.

[7] Ormeni Rr., Hoxha I., Naco P., Dashamir G. The strong earthquake of 26 November 2019 (Mw 6.4) and its associate active tectonic of Durresi region in Albania, European Geosciences Union, General Assambly, (EGU2020), Vienna, Austria, 2020.

[8] Öztürk S., Şahin Ş. A statistical space-time-magnitude analysis on the aftershocks occurrence of the July 21th, 2017 M_W=6.5 Bodrum-Kos, Turkey, earthquake, Journal of Asian Earth Sciences, 172 443-457, 2019.

[9] Ranalli G.A Statistical Study of Aftershock Sequences, Annals of Geophysics, 22 359-397, 1969.

[10] Wiemer S., Katsumata K. Spatial variability of seismicity parameters in aftershock zones, J. Geophys. Res., 104:B6 13135-13151, 1999.

[11] Ogata Y. Increased probability of large earthquakes near aftershock regions with relative quiescence, J. Geophys. Res., 106 8729-8744, 2001.

[12] Polat O., Eyidogan H., Haessler H., Cisternas A., Philip H. Analysis and interpretation of the aftershock sequence of the August 17, 1999, Izmit (Turkey) earthquake, Journal of Seismology, 6 287-306, 2002.

[13] Bayrak Y., Öztürk S. Spatial and temporal variations of the aftershock sequences of the 1999 İzmit and Düzce earthquakes, Earth Planets and Space, 56:10 933-944, 2004.

[14] Öztürk S., Çınar H., Bayrak Y., Karslı H., Daniel G. Properties of Aftershock Sequence of the 2003 Bingöl, M_D=6.4, (Turkey) Earthquake, Pure and Applied Geophysics, 165:2 349-371, 2008.

[15] Enescu B., Enescu D., Ito K. Values of b and p: Their variations and relation to physical processes for Earthquakes in Japan and Romania, Romanian Journal of Physics, 56:3-4 590-608, 2011.

[16] Zhang S., Wang G., Sa W. Damage evaluation of concrete gravity dams under mainshock–aftershock seismic sequences, Soil Dynamics and Earthquake Engineering, 50 16-27, 2013.

[17] Nemati M. An appraisal of aftershocks behavior for large earthquakes in Persia, Journal of Asian Earth Sciences, 79 432-440, 2014.

[18] Ávila-Barrientos L., Zúñiga F.R., Rodríguez-Perez Q., Guzmán-Speziale M. Variation of b and p values from aftershocks sequences along the Mexican subduction zone and their relation to plate characteristics, Journal of South American Earth Sciences, 63 162-171, 2015.

[19] Ansari S. Aftershocks properties of the 2013 Shonbe Mw 6.3 earthquake, central Zagros, Iran, Journal of Asian Earth Sciences, 147 17-27, 2017.

[20] Ormeni Rr., Öztürk S. A statistical analysis on the aftershock sequence for July 3rd, 2017, border region of Macedonia-Albania (M_L=5.0) earthquake: Aftershock probability evaluation, Journal of Natural and Technical Sciences, XXIII(47) 95-110, 2018.

[21] Ormeni Rr., Öztürk S. An appraisal on the aftershock characteristics of the July 4, 2018 earthquake, M_L=5.1, near Durrës, Albania, Journal of Natural and Technical Sciences, XXIV(48) 27-44, 2019.

[22] Nanjo K.Z. Were changes in stress state responsible for the 2019 Ridgecrest, California, earthquakes? Nature Communications, 11 3082, 2020.

[23] Utsu T.A Statistical study on the occurrence of aftershocks, Geophys. Mag., 30 521-605, Tokyo, Japan, 1961.

[24] Gutenberg R., Richter C.F. Frequency of earthquakes in California, Bull. Seismol. Soc. Am., 34 185-188, 1944.

[25] Öncel A.O, Main I., Alptekin A., Cowie P. Spatial variations of the fractal properties of seismicity in the Anatolian fault zones, Tectonophysics, 257 189-202, 1996.

[26] Wiemer S.A software package to analyze seismicity: ZMAP, Seismol. Res. Lett., 72:2 373-382, 2001.

[27] Ormeni Rr. Structure of P, S seismic wave velocities of the Albanian earth lithospheres and its seismoactive features, Kumi publications, Tirana, 2010.

[28] Klein F.W. User's guide to HYPOINVERSE-2000, a Fortran program to solve for earthquake locations and magnitudes, U.S. Geological Survey, Menlo Park, CA, 2002.

[29] Grassberger P., Procaccia I. Measuring the strangeness of strange attractors, Physics, D9 189-208, 1983.

[30] Utsu T., Ogata Y., Matsu'ura R.S. The centenary of the Omori formula for decay law of aftershock activity, J. Phys. Earth, 43 1-33, 1995.

[31] Utsu T. Aftershock and earthquake statistic (III): Analyses of the distribution of earthquakes in magnitude, time and space with special consideration to clustering characteristics of earthquake occurrence (1), J. Faculty Sci., Hokkaido University, Ser., VII (Geophys.) 3 379-441, 1971.

[32] Frohlich C., Davis S. Teleseismic b-values: Or, much ado about 1.0, J. Geophys. Res., 98:B1 631-644, 1993.

[33] Hirata T. Aftershock sequence of the earthquake off Shikotan Island on January 29, 1968, Geophys. Bull. Hokkaido Univ., 21 33-43, 1969.

[34] Öncel A.O., Wilson T.H. Space-time correlations of seismotectonic parameters and examples from Japan and Turkey preceding the İzmit earthquake, Bull. Seismol. Soc. Am., 92 339-350, 2002.

[35] Polat O., Gok E., Yılmaz D. Earthquake hazard of the Aegean Extension region (West Turkey), Turkish Journal of Earth Sciences, 17 593-614, 2008.

[36] Wiemer S., Wyss M. Minimum magnitude of completeness in earthquake catalogs: Examples from Alaska, the Western United States, and Japan, Bull. Seismol. Soc. Am., 90:3 859-869, 2000.

[37] Ogata Y. Estimation of the parameters in the modified Omori formula for aftershock frequencies by the maximum likelihood procedure, J. Phys. Earth., 31 115-124, 1983.

[38] Aki, K. Maximum likelihood estimate of *b* in the formula log$N$ =a-bM and its confidence limits, Bull. Earthquake Res. Inst., Tokyo University, 43 237-239, 1965.

[39] Helmstetter A., Shaw B. Relation between stress heterogeneity and aftershock rate in the rate-and-state model, J. Geophys. Res., 111 B07304, 2006.

[40] Peng Z., Vidale J.E., Ishii M., Helmstetter A. Seismicity rate immediately before and after mainshock rupture from high-frequency waveforms in Japan, J. Geophys. Res., 112 B03306, 2007.

[41] Kisslinger C., Jones L.M. Properties of aftershock sequences in Southern California., J. Geophys. Res., 96:B7 11,947-11,958, 1991.